JOINT INSTITUTE FOR AERONAUTICS AND ACOUSTICS

National Aeronautics and
Space Administration

Ames Research Center

JIAA TR - 95

Stanford University

ASYMPTOTIC BEHAVIOR OF A FLAT PLATE WAKE

By

James H. Weygandt and Rabindra D. Mehta

Stanford University
Department of Aeronautics and Astronautics
Stanford, CA 94305

SEPTEMBER 1989

ABSTRACT

An experimental study has been conducted to investigate the far-field, self-similar properties of a flat plate wake. A plane turbulent wake was generated at the trailing edge of a smooth splitter plate separating two legs of a Mixing Layer Wind Tunnel, with both initial boundary layers tripped. For the present study, both legs were operated at a free-stream velocity in the test section of 15 m/s, giving a Reynolds number based on wake momentum thickness of about 1750. Single profile measurements were obtained at five streamwise locations using a pitot probe for the mean velocity measurements and a single cross-wire probe for the turbulence data, which included statistics up to third order. The mean flow data indicated a self-similar behavior beyond a streamwise distance equivalent to about 350 wake momentum thicknesses. However, the turbulence data show better collapse beyond a distance equivalent to about 500 momentum thicknesses, with all the measured peak Reynolds stresses achieving constant, asymptotic levels. The asymptotic mean flow behavior and peak primary stress levels agree well with theoretical predictions based on a constant eddy viscosity model. The present data also agree reasonably well with previous measurements, of which only one set extends into the self-similar region. Detailed comparisons with previous data are presented and discussed in this report.

NOMENCLATURE

b:	Wake half-width
C_f:	Boundary Layer skin friction coefficient
H:	Boundary layer shape factor
Re_L:	Reynolds number, UL/ν
R_{uv}:	Shear correlation coefficient
U, V, W:	Mean velocity in the X,Y,Z directions, respectively
U_c:	Centerline velocity in wake
U_0:	Velocity defect in wake
U_e:	Free-stream velocity in the wind tunnel
U_τ:	Friction velocity
u', v', w':	Fluctuating velocity components in the X,Y,Z directions, respectively
u, v, w:	Instantaneous velocity in the X,Y,Z directions, respectively, e.g. u = U + u'
X, Y, Z:	Cartesian coordinates for streamwise, normal, and spanwise directions, respectively
Y_c:	Centerline of wake
δ_{99}:	Initial boundary layer thickness
ν:	Kinematic viscosity of air
θ:	Far-field momentum thickness of wake
θ_0:	Initial boundary layer momentum thickness
ρ:	Density of air
$\overline{\quad}$:	(overbar) Time-averaged quantity
$()_{max}$:	Maximum value at given X-station

1. INTRODUCTION

The turbulent plane wake represents an important area of study because of its applications to various facets of aerodynamics and hydrodynamics. An understanding of the flow in the wake is essential to the prediction of performance of important practical elements, such as airfoils and turbine blades. This is due to the fact that the pressure distributions over the rear part of the elements are affected by a complex interaction involving the boundary layers, wake and the external potential flow field. The behavior of the wake is also of significance for multi-element airfoils, in which the wake of one element may interact with the boundary layer of another. Similarly, the far-wake flow is of interest since the wake shed by the canard or the main wing may then interact with elements further downstream, such as the tailplane. Despite the importance of the plane wake in practical aerodynamics, relatively few studies of its *complete* evolution have been conducted.

Most of the earlier work on plane wakes concentrated on circular cylinder wakes, the most notable amongst which was that due to Townsend (1947). It was these results, together with data from other free-shear flows that led to the concept of self-similarity (Townsend, 1956). It was proposed that sufficiently far downstream of the origin, the flow becomes fully independent of the initial conditions and achieves an asymptotic, self-similar state whereby its development can be described by a single, *local* velocity and length scale. In particular, the Reynolds stresses should become independent of streamwise location when normalized by the velocity scale — the peak values of the normalized Reynolds stresses should therefore achieve constant values . However, recent investigations have suggested that while the mean flow may become self-similar, universality is not observed for wakes generated by different bodies and thus, the asymptotic turbulence structure is still dependent on the initial conditions (Wygnanski *et al.* 1986). These results, therefore, suggest that wakes generated by different bodies should perhaps be studied individually.

The simplest, and by far the most popular, way of generating a plane wake, which adequately simulates an airfoil wake, is by using a flat, smooth plate at zero angle of attack. A geometrically two-dimensional, straight and symmetric wake can then be easily generated. Also, a relatively long flat plate enables the generation of thick, well-behaved turbulent boundary layers which can be accurately documented.

One of the first experimental investigations of a flat plate wake was that due to Chevray and Kovasznay (1969). They obtained mean flow and turbulence data up to X/θ = 414. They noted that the early development of the wake was different to that for a bluff body wake and also discussed the fact that the turbulence intensity distributions developed two peaks, in the regions of maximum mean shear. The only experimental investigation in which the complete evolution of the wake, from the very near-field to the self-similar far-field, was studied in any detail appears to be that by Pot (1979). Although Pot presented a lot of data in his report, there was not much attempt at analyzing or discussing the results. In fact, it was not until some years later that his data was put into perspective by Ramaprian *et al.* (1982).

Ramaprian *et al.* (1982) were one of the first investigators to divide the wake into three distinct regions. The near-wake region extends from the trailing edge to approximately X/θ = 25. The near-wake is governed by the near-wall region of the boundary layer upstream

of the trailing edge and is characterised by the presence of an inner wake. This region is characterised by fine-scale mixing between the boundary layers merging from the two sides of the plate. The intermediate-wake extends from $X/\theta = 25$ to 350, and in this region, the influence of the upstream boundary layer is insignificant and the wake evolves as a free-turbulent flow because the inner wake has absorbed the log-region of the boundary layers. In this region there are two turbulence structures, one related to the inner-wake resulting from small-scale mixing and the other resulting from the large-scale structures of the outer boundary layer, which approaches the final structure characteristic of the far-wake. The far-wake region extends beyond $X/\theta = 350$, and the flow in this region attains a self-similar form when the wake half-width, b, and velocity defect, U_0, exhibit asymptotic behavior in the form of:

$$b \propto (X)^{1/2} \qquad U_0 \propto (X)^{-1/2} \tag{1}$$

Ramaprian *et al.* (1982) showed that thier near-field data agreed well those of Pot's (1979) and also demonstrated that Pot's far-field results agreed reasonably well with theretical predictions given by a constant eddy viscosity model.

Other experimental studies have either restricted their attention to the very near-wake (Nakayama and Liu 1987) or the turbulence structure in the near-wake using conditional sampling techniques (Andreopolous & Bradshaw 1980 and Jovic & Ramaprian 1986). Numerous analytical studies of turbulent wakes of flat plates have also been conducted. Alber (1979) developed an analytical solution for the near-wake region and compared this solution to the data of Chevray and Kovasznay (1969). Patel and Chen (1986) solved numerically the flow from the boundary layer of a flat plate through the interaction zone into the far-wake and found satisfactory agreement with experiments in all regions except for underestimating the growth of the far-wake.

The present study was motivated by the sparsity of data for the far-wake, in particular. The main objective of this experiment was to provide a set of far-field data for comparison with the data of Pot (1979) and with theoretical predictions.

2. EXPERIMENTAL APPARATUS AND TECHNIQUES

The experiments were conducted in the Mixing Layer Wind Tunnel located in the Fluid Mechanics Laboratory at NASA Ames Research Center (Fig. 1). The wind tunnel consists of two separate legs which are driven individually by centrifugal blowers connected to variable speed motors. The two streams are allowed to merge at the sharp edge of a slowly tapering splitter plate; the included angle at the splitter plate edge, which extends 15 cm into the test section, is about 1°. The test section is 36 cm in the cross-stream direction, 91 cm in the spanwise direction and 366 cm in length. One side-wall is flexible so that it can be adjusted for streamwise pressure gradient control, although for the present measurements, this wall was kept fixed at a constant distance from the opposite wall. This adjustable side-wall is also slotted for probe access.

For the present experiments, both legs were operated at a free-stream velocity in the test section of 15 m/s. The free-stream velocities were held constant to within 1% during

a typical run lasting two hours. At these operating conditions, the measured streamwise turbulence level (u'/U_e) was about 0.15% and the transverse levels (v'/U_e and w'/U_e) were about 0.05%. The mean core-flow was found to be uniform to within 0.5% and cross-flow angles were less than 0.25°. Further details of the wind tunnel design and flow quality measurements are given in Bell and Mehta (1989). The boundary layers were tripped using a 1.5 mm diameter round wires installed 15 cm upstream of the splitter plate trailing edge. The measured boundary layer properties at the trailing edge are summarized in Table 1. The spanwise variation in skin friction coefficient was found to be less than ±5% for both boundary layers.

Measurements were made using a pitot and a cross-wire probe held on a 3-D traverse and linked to a fully automated data acquisition and reduction system controlled by a MicroVax II computer. The cross-wire probe had 5 μm tungsten sensing elements about 1 mm long and positioned about 1 mm apart. The probe was calibrated statically in the potential core of the flow assuming a 'cosine-law' response to yaw, with the effective angle determined by calibration. The analog signals were filtered (low pass at 30 Khz), DC offset, and amplified (X 10) before being fed into a NASA-built computer interface. The interface contained a fast sample-and-hold A/D converter with 12 bit resolution and a multiplexer for connection to the computer (Westphal and Mehta 1983). Individual statistics were averaged over 5,000 samples obtained at a rate of 400 samples per second.

Turbulence data were obtained in two planes (uv and uw) by rotating the cross-wire probe about its own axis. This method yielded all three components of mean velocity, five independent components of the Reynolds stress tensor and selected higher order products. Data were obtained at five streamwise stations within the test section between X = 93.9 and 1064 θ. Although all of the measurements presented here were obtained on the tunnel centerline, spanwise checks were also made at all stations.

3. RESULTS AND DISCUSSION

The assumptions of self-preservation and small velocity defect result in the half-power laws for half width b and maximum velocity defect U_0. The additional assumption of constant eddy viscosity ν_T across the wake leads to the asymptotic relations for velocity defect U_0 and shear stress $\overline{u'v'}$ given by:

$$U/U_0 = exp(-4\eta^2 ln2) \tag{2}$$

$$\overline{u'v'}/U_0^2 = 8(ln2)(\nu_T/U_0 b)\eta exp(-4\eta^2 ln2) \tag{3}$$

where η = y/b. Based on the wake momentum thickness θ, the explicit growth and decay laws can be expressed as:

$$(U_e/U_0)^2 = 4\pi(\nu_T/U_e\theta)(X/\theta) \tag{4}$$

$$(b/\theta)^2 = 16(\nu_T/U_e\theta)ln2(X/\theta) \tag{5}$$

Townsend (1956) gave a value of 0.032 for $\nu_T/U_e b$, which was later also recommended by Ramaprian *et al.* (1982). Using this value in Eq.(3) suggests that $\overline{u'v'}/U_0^2$ approaches a maximum value of 0.0487 in the far wake. The above expressions are based on the assumption of constant eddy viscosity, and thus may only be approximate, especially towards the outer edges of the wake. They are sufficient, however, for studying the collapse to asymptotic behavior.

The mean velocity data, normalized by the local velocity defect and half-width, are presented in Fig. 2. This figure includes the asymptotic profile given by Eq. (2). Apart from the first profile at $X/\theta = 8.4$, which is still in the near-wake region, all the other downstream profiles seem to follow the asymptotic curve reasonably well. The small discrepancy near the outer edges was also observed in previous studies (Ramaprian *et al.* 1982) and may be attributed to the effects of intermittency which is obviously not accounted for in the constant eddy viscosity model. Based on these data alone, it appears as though the mean flow has achieved self-similarity beyond $X/\theta \geq 122.5$. However, a different conclusion is reached when the streamwise development of the velocity and length scales are examined.

The streamwise developments of the velocity scale (normalized mean velocity defect) and the length scale (normalized half-width) are shown in Figs. 3 and 4, respectively. Also shown in these figures are the data due to Pot (1979) and the asymptotic behavior given by Eqs. (4) and (5). A least-squares best fit is also included for each experimental data set. For the present data, a linear behavior is observed for both quantities only beyond $X/\theta \sim 350$, thus indicating that even the mean flow does not achieve self-similarity upstream of this station, as suggested by the data in Fig. 2. Pot's data also shows a linear behavior in this region, although the slopes are slightly different from the current ones. On the whole, both experimental data sets agree reasonably well with the theoretical predictions, although the difference in slopes is somewhat smaller for the present data.

The measured profiles for the three Reynolds normal stresses ($\overline{u'^2}$, $\overline{v'^2}$ and $\overline{w'^2}$) are plotted in similarity coordinates in Figs. 5, 6 and 7, respectively. The results for $\overline{u'^2}$ and $\overline{w'^2}$ are qualitatively similar, in that they have a double-peaked distribution, with the peaks reasonably symmetric, except for the $X/\theta = 750.4$ profile in Fig. 5. This type of double-peaked distribution is not altogether surprising since the peaks coincide with the two regions of maximum mean streamwise velocity gradient, and hence regions of maximum turbulence production, in the wake. The $\overline{v'^2}$ profiles in the very near-wake measured previously also show a double-peaked distribution (Pot 1979 and Jovic & Ramaprian 1986). However, the double-peaks are quickly "washed-out" giving a single-peaked distribution as is evident in Fig. 6. This is probably caused by an effective "meander" of the wake (in the vertical direction) as seen by a stationary probe since the streamwise structure of the wake appears snake-like due to the presence of opposite-signed vorticity. For self-similarity, the Reynolds stress profiles and peak levels are expected to collapse when plotted in these similarity coordinates and this appears to be the case for at least the last two streamwise locations.

The primary shear stress $\overline{u'v'}$ profiles, presented in Fig. 8, also show a double-peaked distribution, but of opposite, in accordance with the change of sign in the mean velocity gradient. Once again, the profiles appear reasonably symmetric and the profiles for the

last two or three locations also collapse reasonably well on the theoretical asymptotic curve given by Eq. (3), thus indicating a self-similar behavior beyond $X/\theta \sim 500$.

The triple products ($\overline{u'^2v'}$ and $\overline{u'v'^2}$, which represent transport of the Reynolds stresses are plotted in Figs. 9 and 10. Once again, the triple products exhibit good symmetry for all profiles and reasonable collapse for the ones at the last three stations. The collapse of the triple products is a strong and relevant indicator for self-similarity since the higher-order products will, in general, take longer to achieve an asymptotic behavior.

In order to investigate the approach to self-similarity in a more quantitative manner, the streamwise development of the peak measured Reynolds stresses and tripe products is plotted in Figs. 11 - 16. For profiles with multiple peaks, the maxima were averaged over two peaks for $\overline{u'^2}$, $\overline{w'^2}$ and $\overline{u'v'}$ and $\overline{u'^2v'}$ and over the three peaks for $\overline{u'v'^2}$. Also included in the plots are available data from previous investigations averaged in the same way. The peak normal stresses measured in the present study all seem to asymptote to constant levels beyond $X/\theta \sim$ 500-600 (Figs. 11, 12 and 13). However, Pot's (1979) peak levels in the far-wake are significantly higher than the present data, and also do not show a consistent levelling-off trend, especially for $\overline{u'^2}$ which shows a monotonic increase, even towards the end of the measurement domain. In the near-field, though, Pot's (1979) data agrees well with that of Jovic & Ramaprian 1986 (Figs. 11 and 12). The peak primary shear stress data from the present study are presented in Fig. 14, together with results from several previous investigations. Also shown in this figure, is the asymptotic maximum level given by Eq. (3). The present data seems to reach a constant level beyond $X/\theta \sim 500$, although the asymptotic level is slightly lower than the theoretical one. Pot's (1979) data also appears to level-off at about the same value at $X/\theta \sim 350$, but then shows a sudden dip followed by a monotonic increase beyond $X/\theta \sim 600$. All of the previous data, obtained in the near-field, seems to agree better with the present trends than with those in Pot's (1979) data. Perhaps the ultimate test of self-similarity is to examine the development of the maximum triple products (Figs. 15 and 16). Both triple products indicate an approximately asymptotic behavior for $X/\theta \geq 500$, or so. The near-field trends also seem to compare well with the data due to Jovic and Ramaprian (1986).

In the boundary layer, upstream of the splitter plate edge, the streamwise fluctuation $\overline{u'^2}$ is expected to be much larger than the normal fluctuation $\overline{v'^2}$, which is constrained by the wall. However, downstream in the wake region, the flow is expected to become more isotropic, as the velocity defect, and hence the associated mean flow gradients become weaker with increasing downstream distance. The streamwise development of the anisotropy parameter ($\overline{u'^2}/\overline{v'^2}$) is shown in Fig. 17. Pot's (1979) and Jovic and Ramaprian's (1986) results show a faster approach to isotropy than the present measurements, although Pot's data also shows an increase in the anisotropy parameter in the far-field ($X/\theta \geq 500$).

On the whole, both Pot's (1979) data and the present results show a self-similar behavior in the far-field. In both studies, the mean flow exhibits a self-similar behavior for $X/\theta \geq 350$. The streamwise development of the wake defect and half-width agrees well with theoretical predictions in this region. It is, however, essential to investigate the turbulence data in order to confirm self-similarity. Based on Pot's (1979) peak shear stress data, Ramaprian *et al.* (1982) concluded that the wake indeed achieved self-similarity at

$X/\theta = 350$. However, on examining the data for all the peak Reynolds stresses (Figs. 11-14), it is clear that this value of X/θ is perhaps underestimated. In the present results, *all* the peak Reynolds stresses achieve constant asymptotic levels beyond $X/\theta \sim 500$. In addition, the peak triple products (Figs. 15 and 16) also show an asymptoting trend at about the same streamwise location. Apart from the somewhat odd behavior in Pot's peak shear stress results for $X/\theta \geq 600$ (Fig. 14), his other normal stresses are not well behaved either (Figs. 11, 12 and 13). In particular, the peak $\overline{u'^2}$ and $\overline{w'^2}$ results show an almost monotonic increase, even towards the most downstream stations at $X/\theta \sim 1000$. Furthermore, all of Pot's peak normal stresses in the far-field are significantly higher than the present data. It is worth noting though, that Pot's near-field results agree reasonably well with previous measurements. It is our belief that Pot's far-field data may be affected by the tunnel wall boundary layer. Although the plate generating the wake was placed 19 cm from the tunnel wall, the wake thickness at the last measurement station was about 9 cm and the tunnel wall boundary layer thickness about 4 cm, thus making it possible for potential flow fluctuations (Wood and Westphal 1988) to have effect.

4. CONCLUSIONS

An experimental study has been conducted on the far-field development of a smooth, flat plate symmetric wake. The mean flow profiles collapse onto the asymptotic theoretical curve at a relatively short distance from the splitter plate trailing edge ($X/\theta \sim 120$). However, the wake deficit and half-width follow the expected power laws only downstream of $X/\theta \sim 350$. Furthermore, the turbulence data, which must be examined in order to evaluate true self-similarity, show adequate collapse only beyond $X/\theta \sim 500$. The present primary shear stress data agree reasonably well with Pot's (1979) results, the only other data set available for the far-field of a flat plate wake, and with the predicted maximum level. The maximum normal stresses in the present study also show the expected asymptotic behavior in the self-similar region, but the levels are lower than those measured by Pot (1979). This discrepancy is attributed to a possible interaction of the wake with the wall boundary layer in Pot's set-up.

ACKNOWLEDGEMENTS

We are grateful to Srboljub Jovic for helpful discussions and to Cherry Ogata for help with the data analyses. This work was supported by and conducted in the Fluid Mechanics Laboratory, Fluid Dynamics Research Branch, NASA Ames Research Center under Grant NCC-2-55.

REFERENCES

Alber, I.E., "Turbulent Wake of a Thin, Flat Plate," *AIAA Journal*, Vol. 18, 1980, pp. 1044-1051.

Andreopolous, J. and Bradshaw, P., "Measurement of Interacting Turbulent Shear Layers in the Near Wake of a Flat Plate," *Journal of Fluid Mechanics*, Vol. 100, 1980, pp. 639-668.

Bell, J.H. and Mehta, R.D. 1989 "Three-Dimensional Structure of a Plane Mixing Layer," AIAA Paper 89-0124.

Bell, J.H. and Mehta, R.D. 1989 "Design and Calibration of the Mixing Layer Wind Tunnel," JIAA Report TR-89, Department of Aeronautics and Astronautics, Stanford University, 1989.

Chevray, R. and Kovasznay, L.S.G., "Turbulence Measurements in the Wake of a Thin Flat Plate," *AIAA Journal*, Vol. 7, 1969, pp. 1641-1643.

Jovic, S. and Ramaprian, B.R., "Large-Scale Structure of the Turbulent Wake Behind a Flat Plate," Institute of Hydraulic Research, University of Iowa, Iowa City, IIHR Report No. 298, 1986.

Patel, V.C. and Chen, H.C., "Turbulent Wake of a Flat Plate," *AIAA Journal*, Vol. 14 , 1987, pp. 1077-1085.

Pot, P.J., "Measurments in a 2-D Wake and in a 2-D Wake Merging into a Boundary Layer," Data Report, NLR TR-79063 U, the Netherlands, 1979.

Ramaprian, B.R., Patel, V.C., Sastry, M.S., "The Symmetric Turbulent Wake of a Flat Plate," *AIAA Journal*, Vol. 20, 1982, pp. 1228-1235.

Townsend, A.A. 1956 *Structure of Turbulent Shear Flow* (Cambridge University Press, Cambridge).

Townsend, A.A. 1976 *Structure of Turbulent Shear Flow* (Cambridge University Press, Cambridge).

Westphal, R.V. and Mehta, R.D., "Crossed Hot-Wire Data Acquisition and Reduction System," NASA TM-85871, 1983.

Wood, D.H. and Westphal, R.V. "Measurements of the Free-Stream Fluctuations Above a Turbulent Boundary Layer," *Physics of Fluids*, Vol. 31, pp. 2834-2840, 1988.

Wygnanski , I., Champagne, F., and Marasli, B., "On the Large-Scale Structures in Two-Dimensional, Small-Deficit, Turbulent Wakes," *Journal of Fluid Mechanics*, Vol. 168, pp. 31-71.

Figure 1: Tunnel Schematic and Operating Conditions

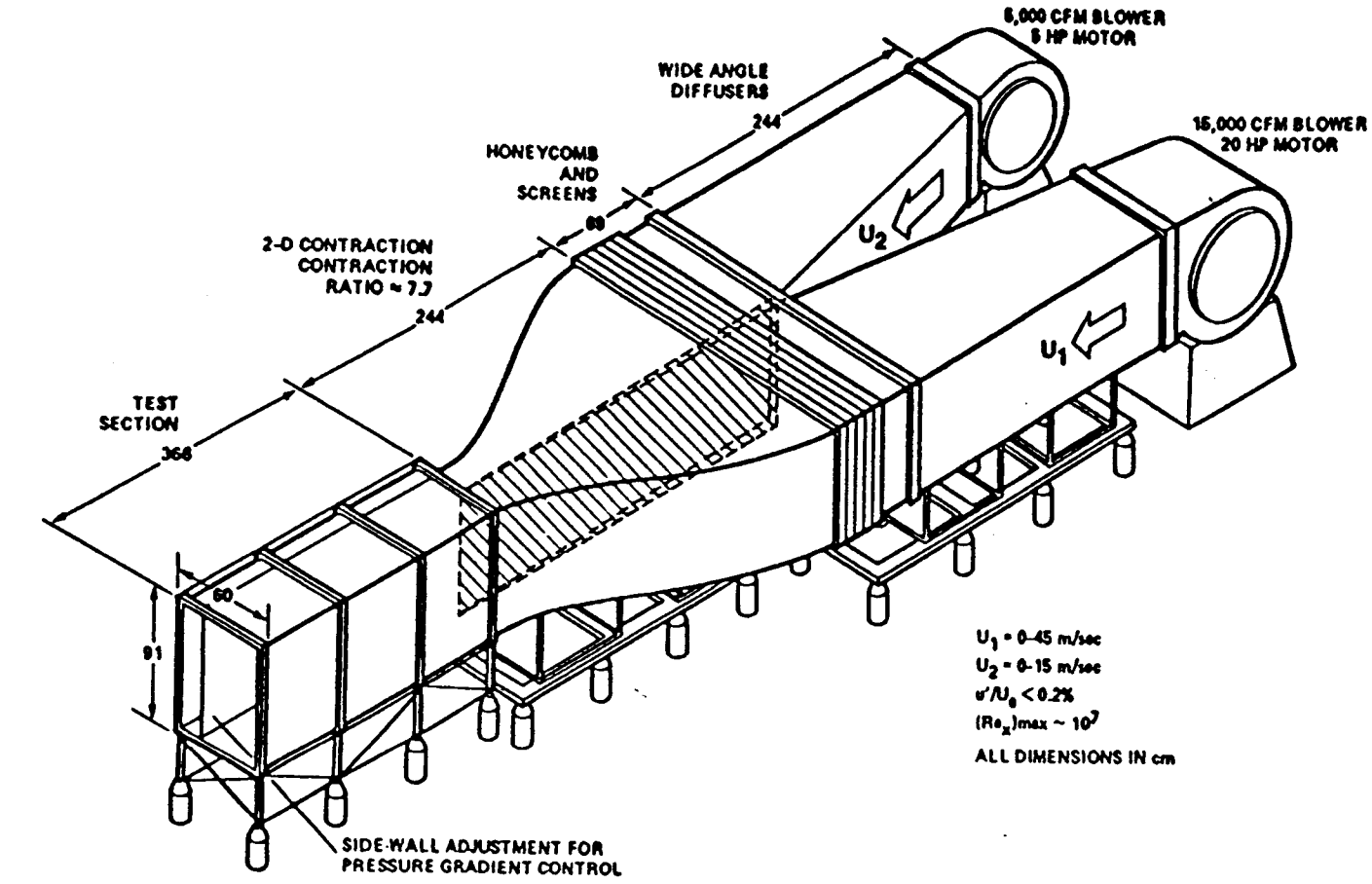

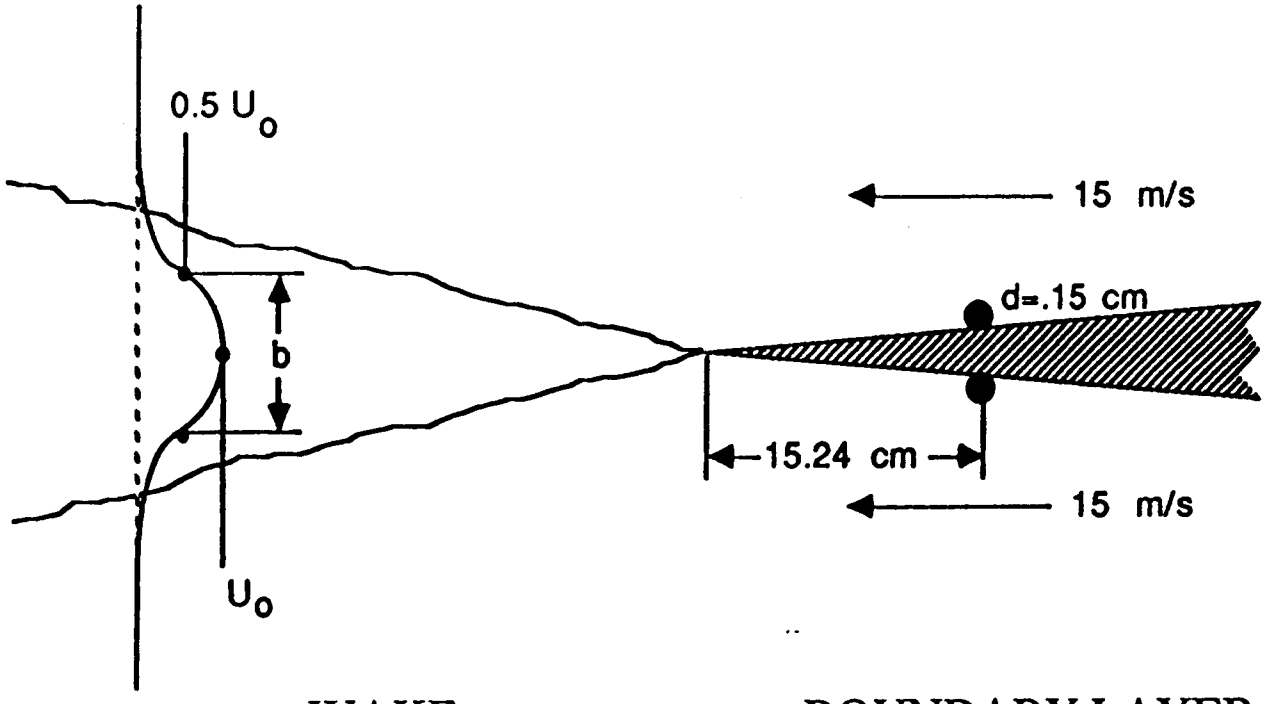

WAKE

$(x)_{max} = 189.4cm$

$(x/\theta)_{max} = 1064$

$Re_\theta = 1750$

$(b)_{max} = 3.43$ cm

BOUNDARY LAYER

$\delta = 85cm$

$\theta_0 = .09$ cm

$C_f = .0048$

$H = 1.46$

Figure 2: Velocity Defect in Local Coordinates

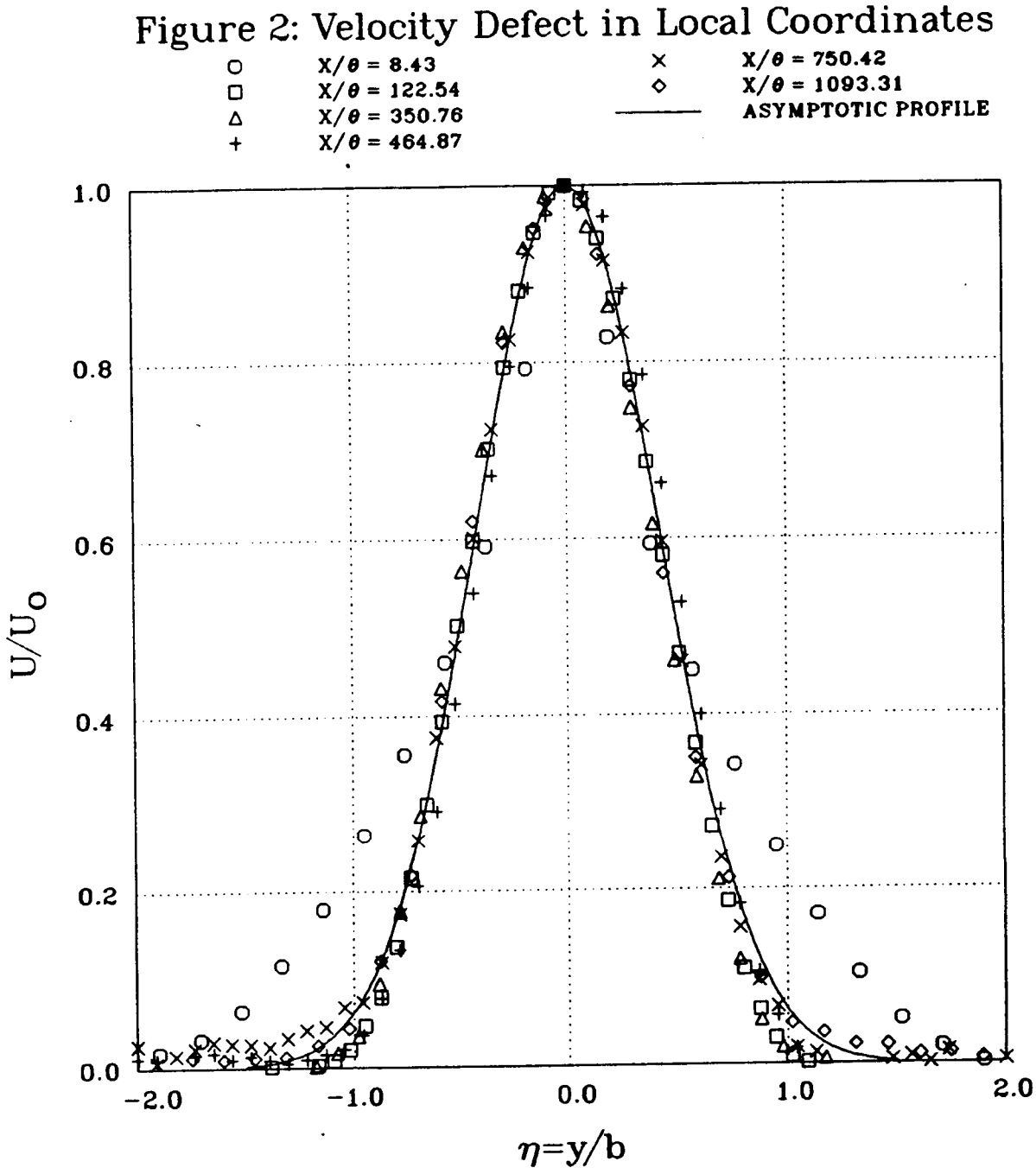

Figure 3: Non−Dimensional Deficit

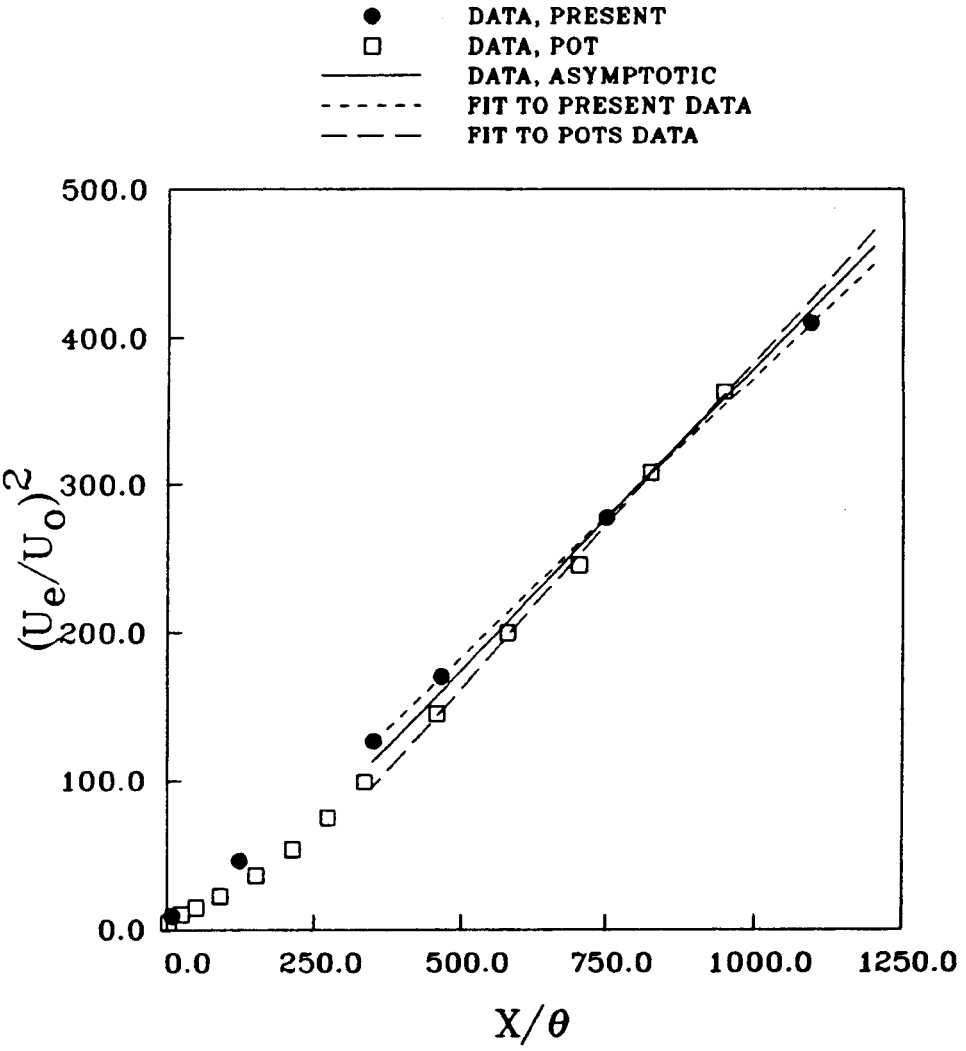

Figure 4: Non−Dimensional Width

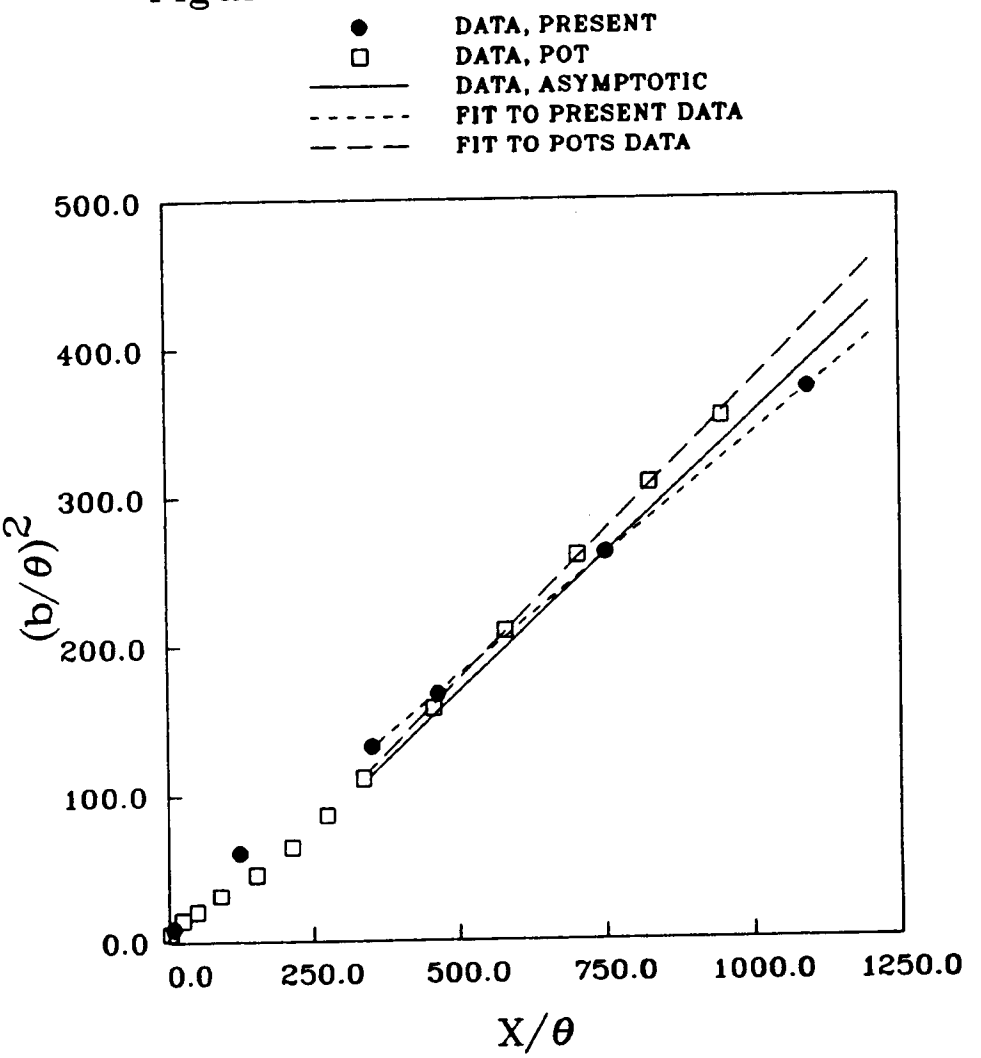

Figure 5: Plot of Streamwise Fluctuation Profiles

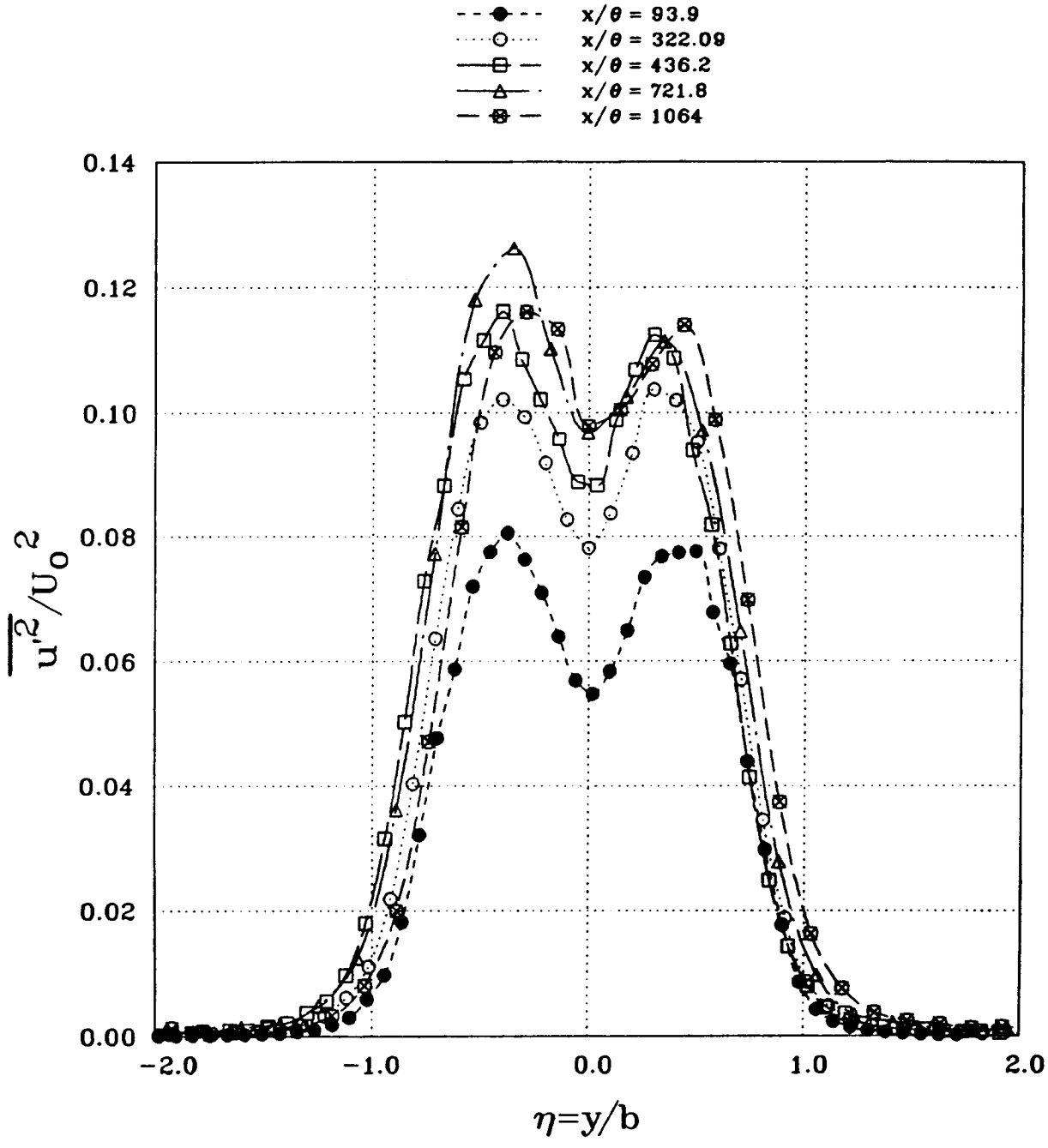

Figure 6: Plot of Normal Fluctuation Profiles

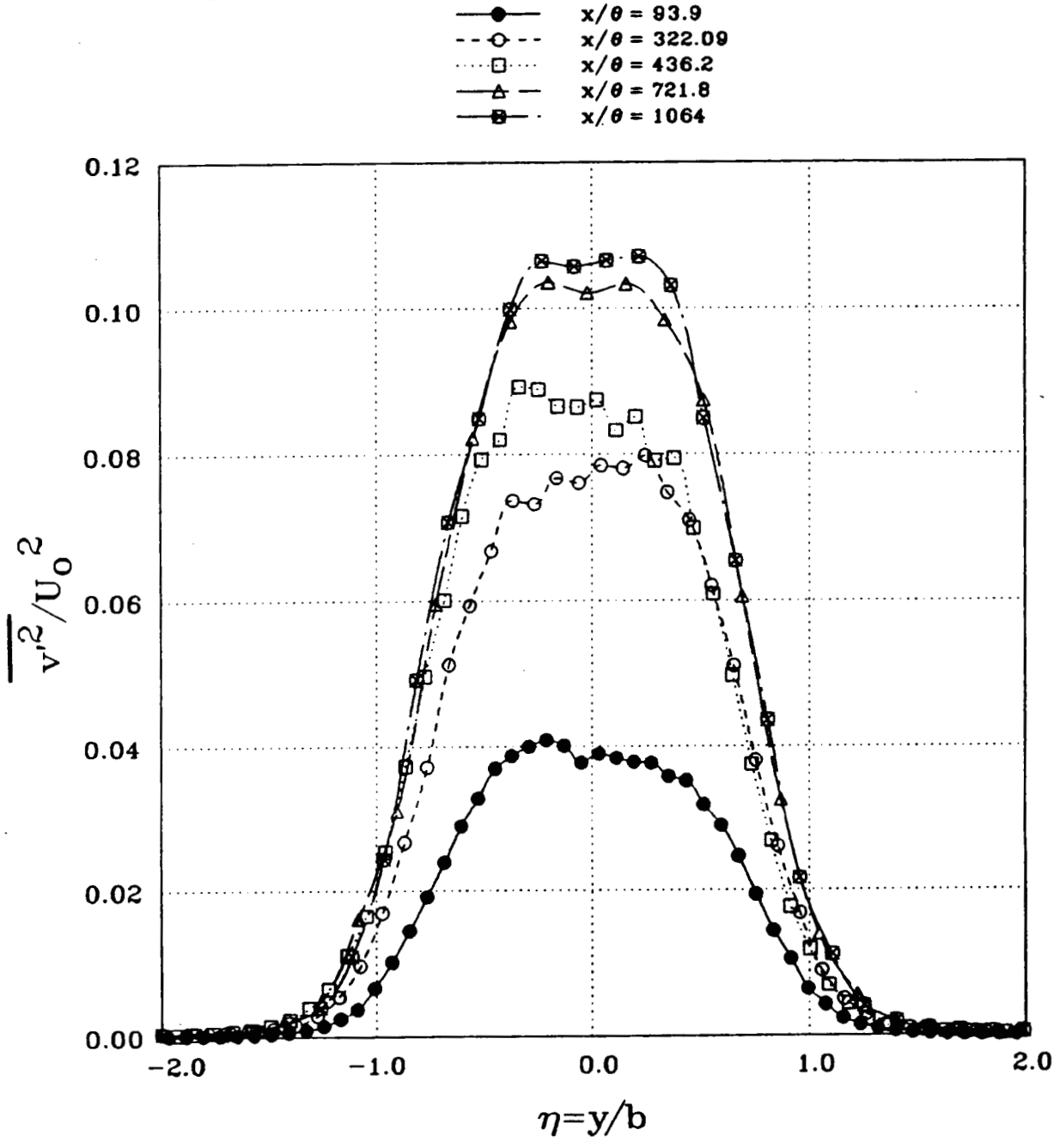

Figure 7: Plot of Spanwise Fluctuation Profiles

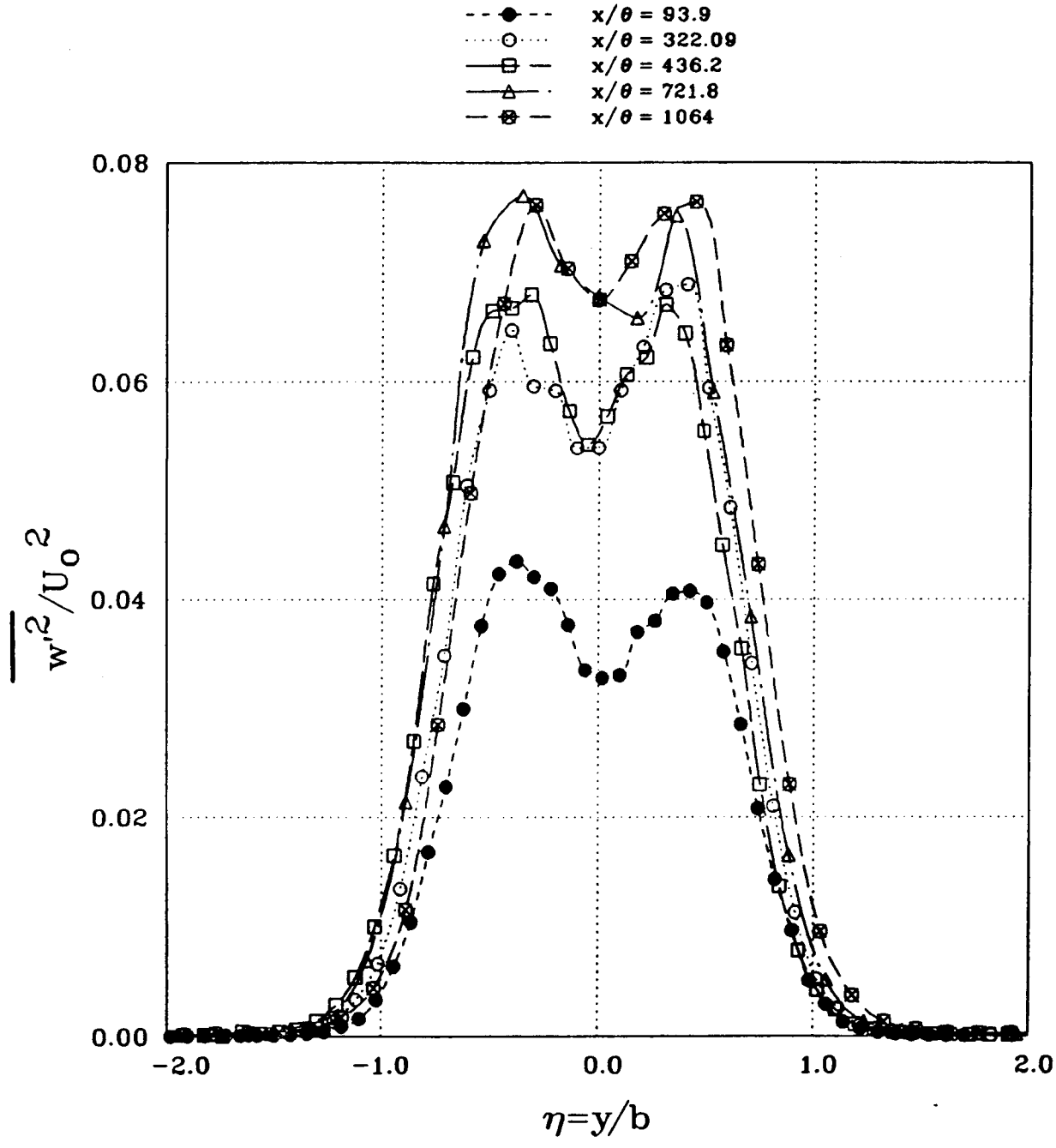

Figure 8: Plot of Primary Shear Stress Profiles

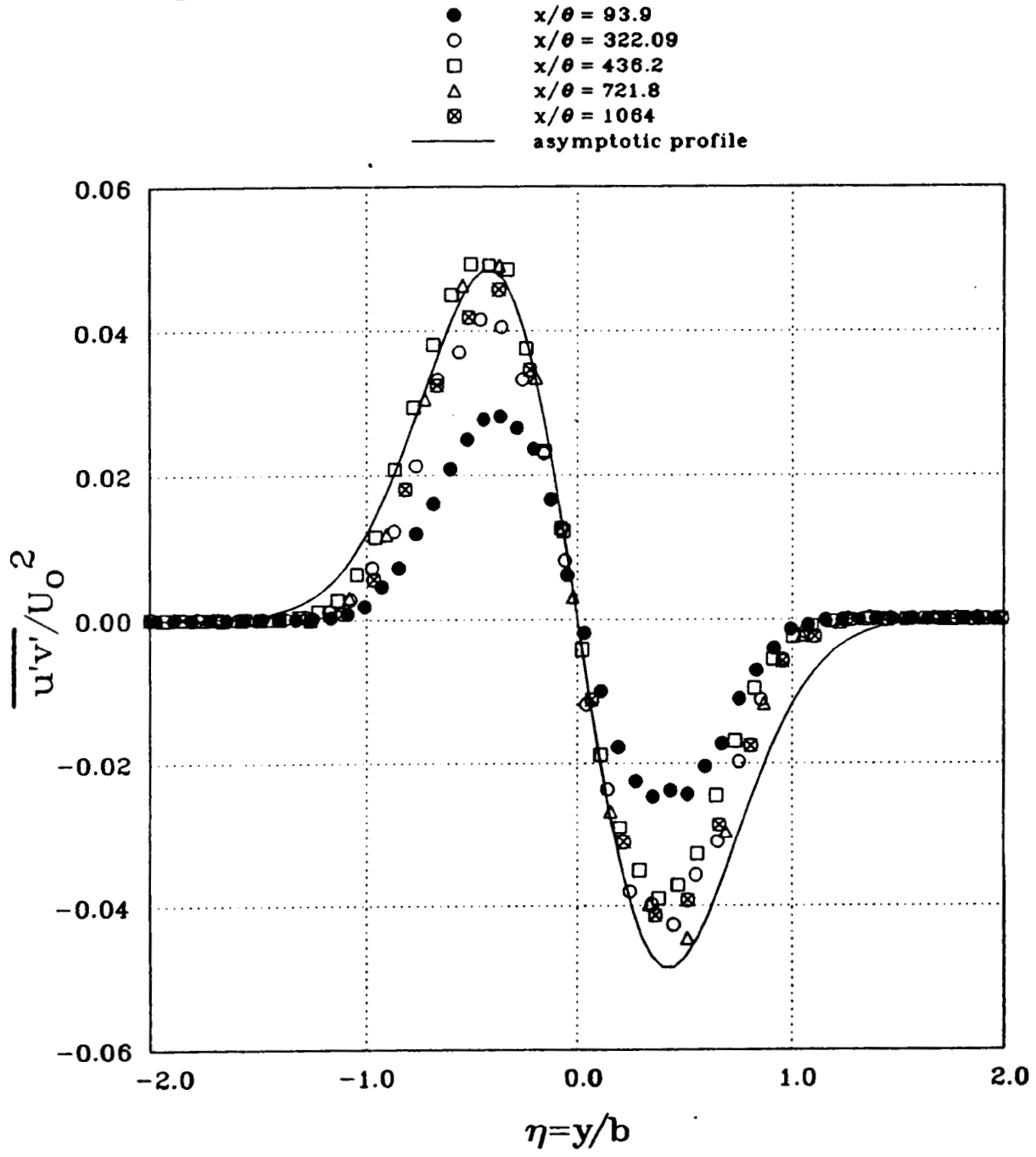

Figure 9: Plot of Triple Product Profiles

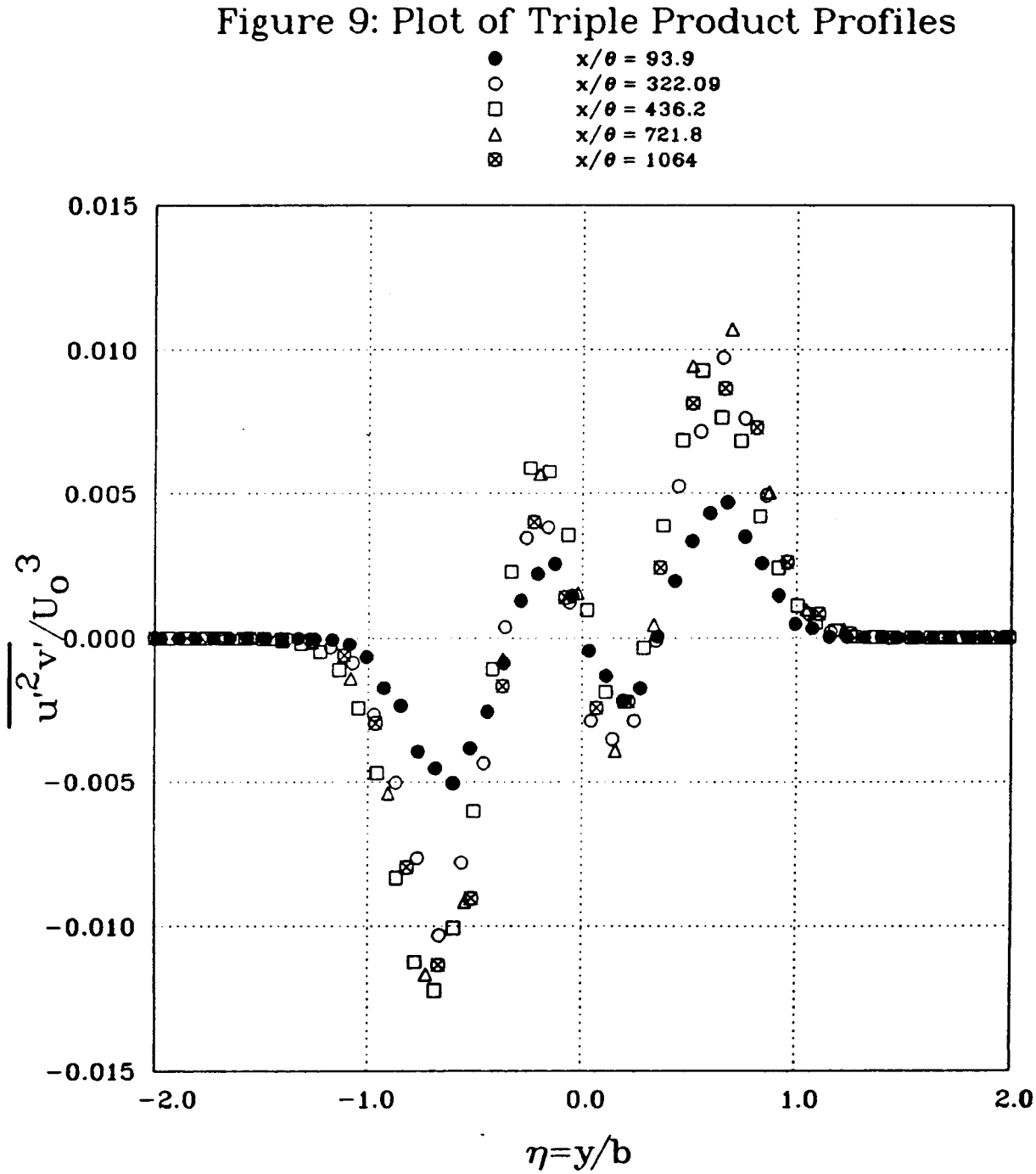

Figure 10: Plot of Triple Product Profiles

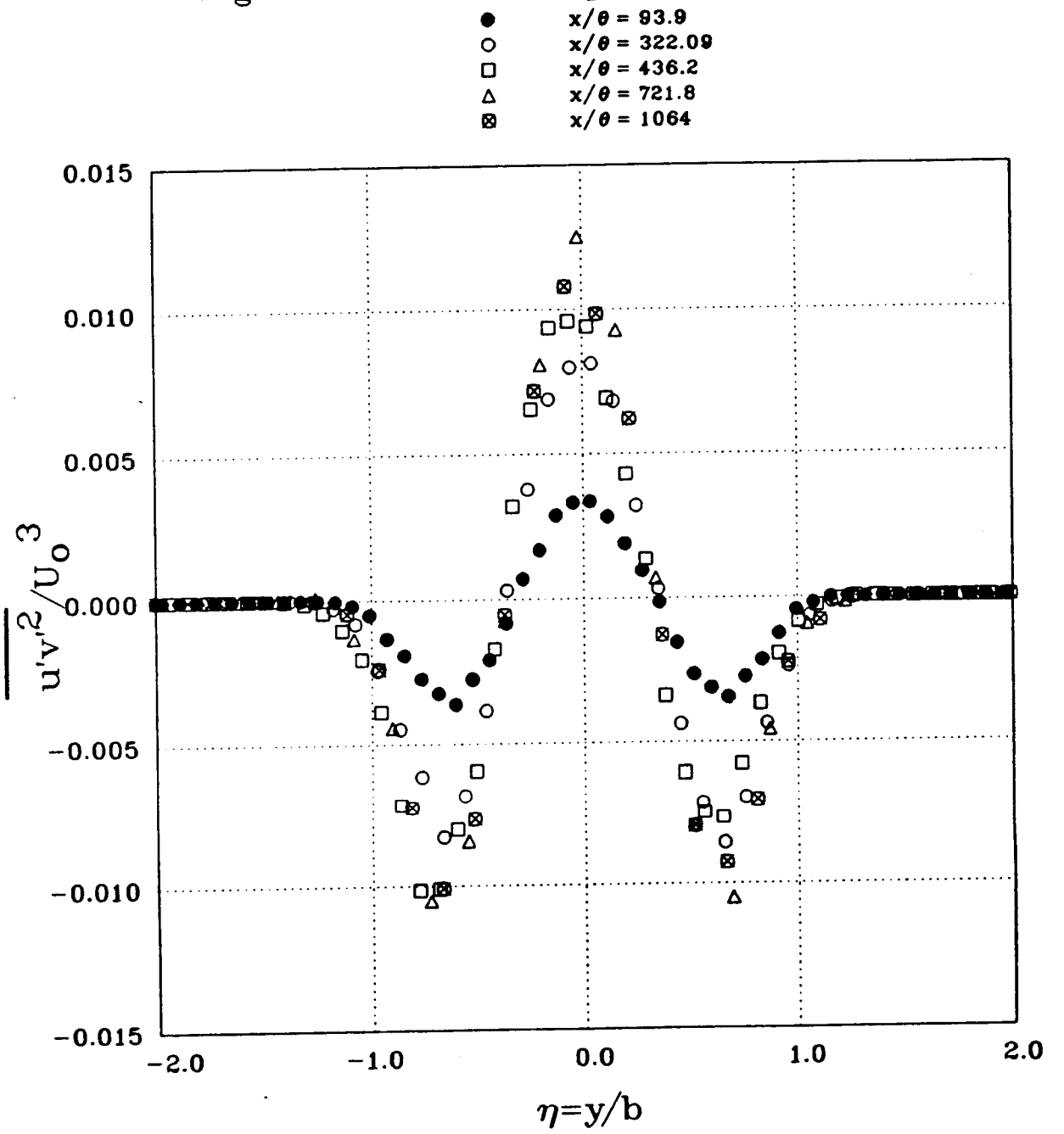

Figure 11: Plot of Maximum Fluctuation Profiles

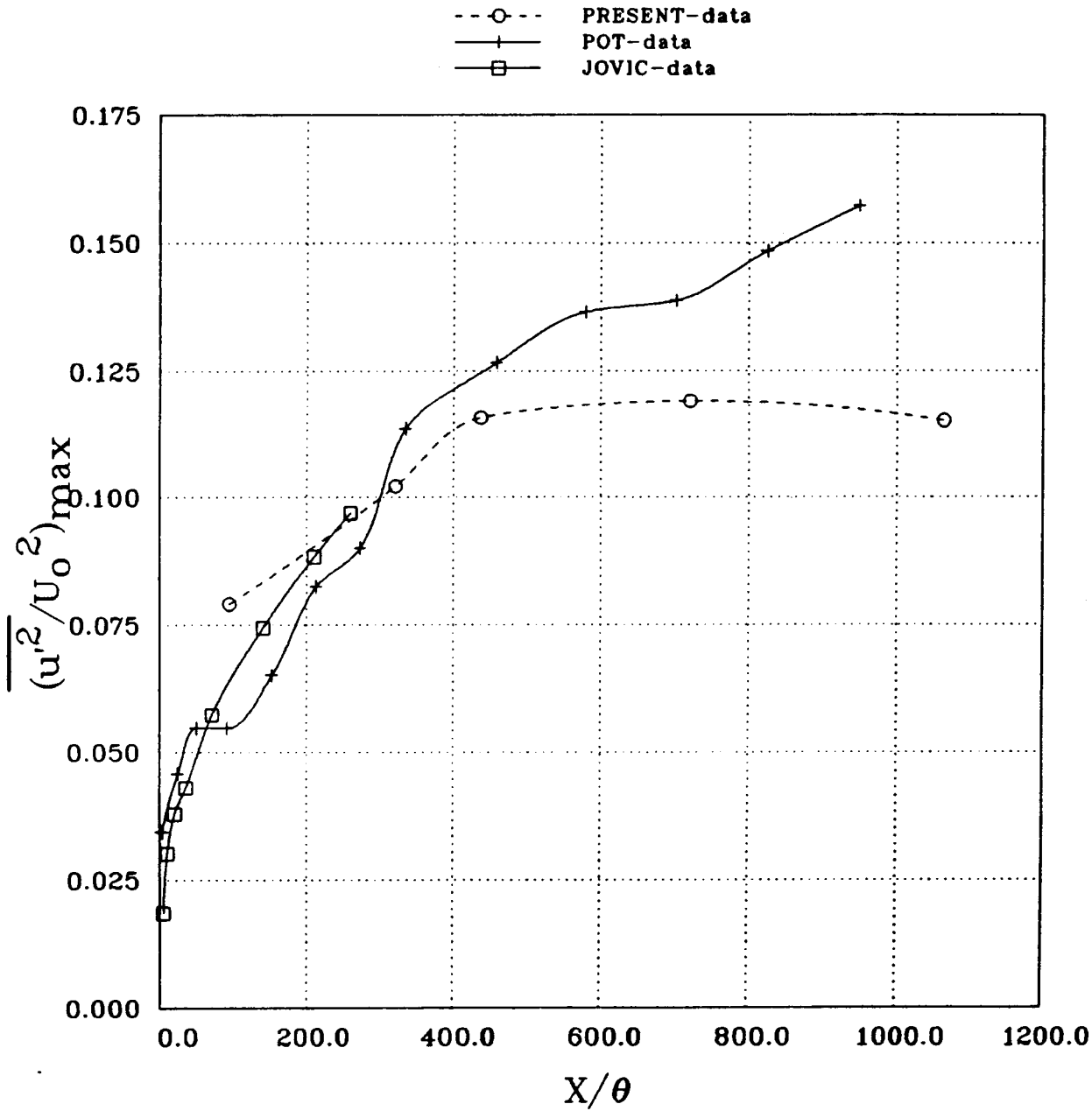

Figure 12: Plot of Maximum Fluctuation Profiles

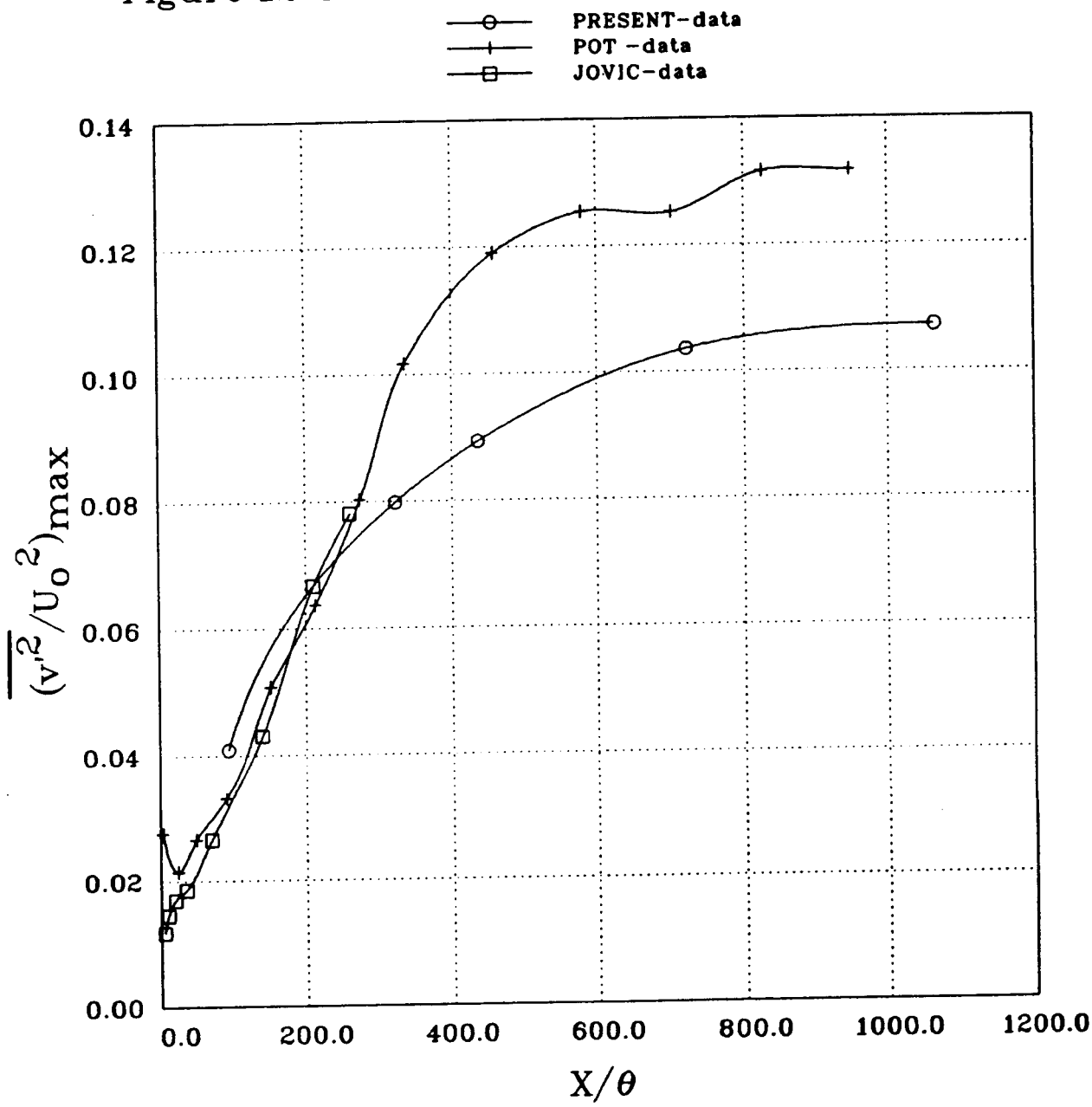

Figure 13: Plot of Maximum Fluctuation Profiles

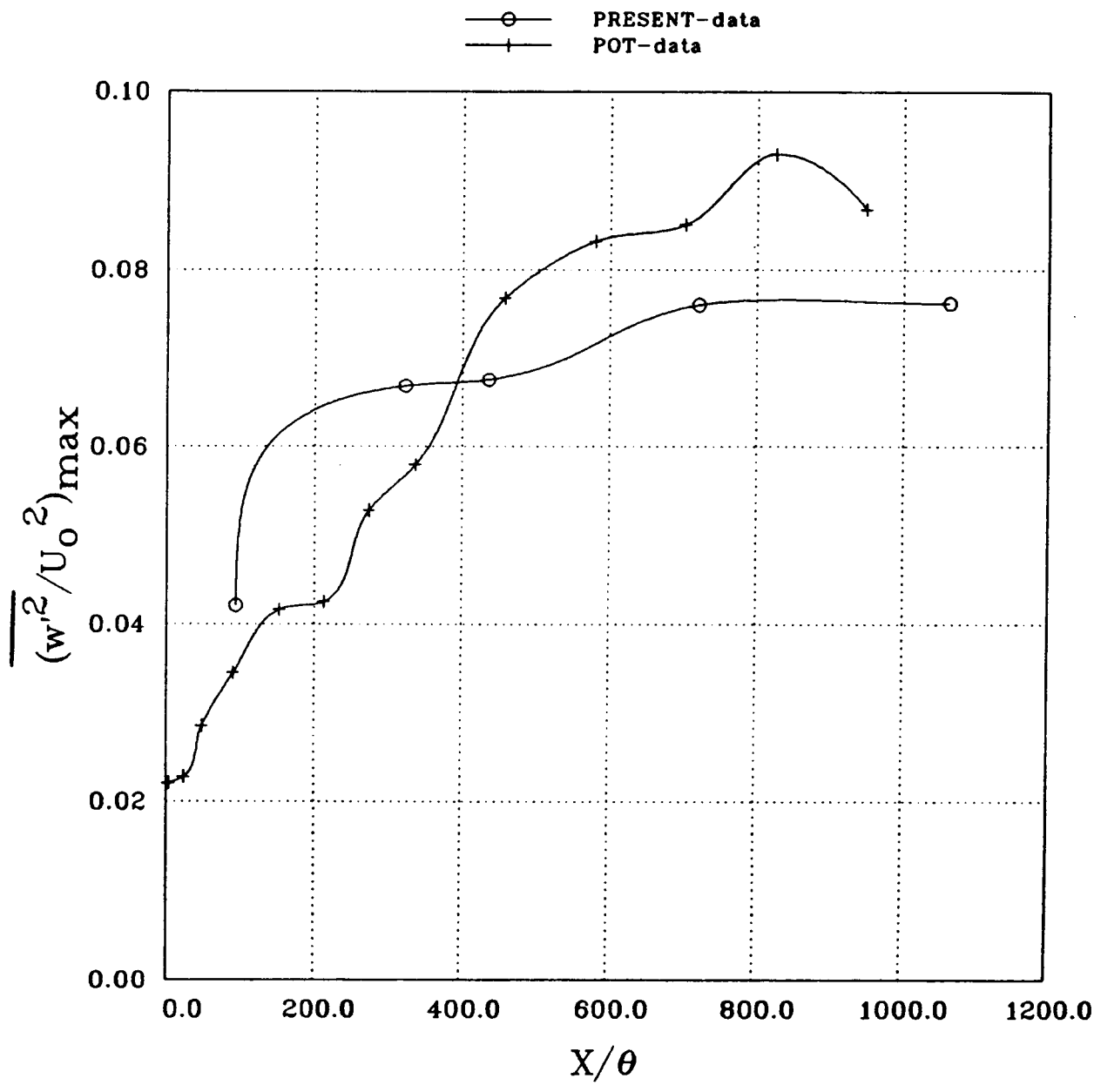

Figure 14: Plot of Maximum Shear Stress Profiles

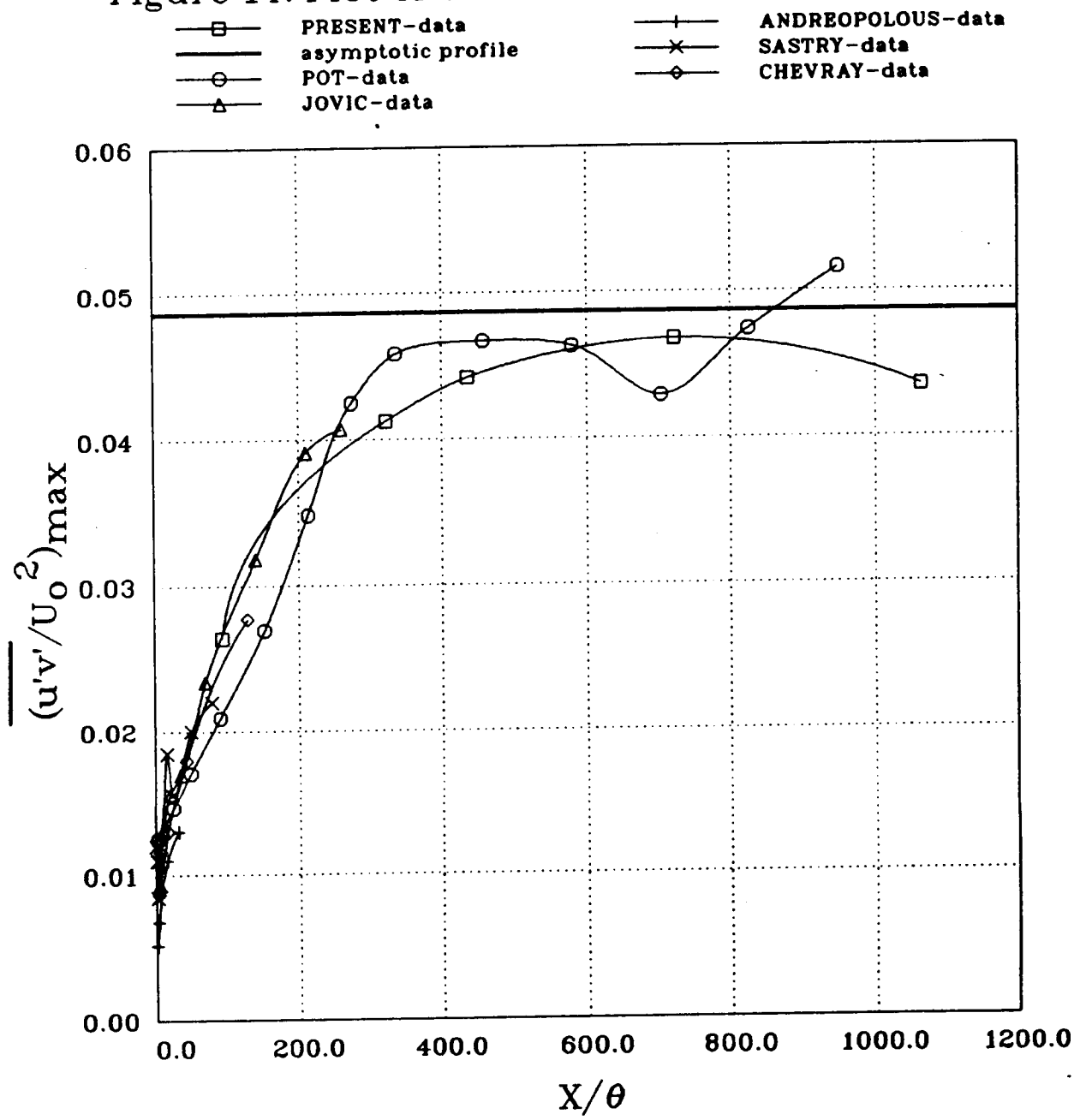

Figure 15: Plot of Maximum Triple Products

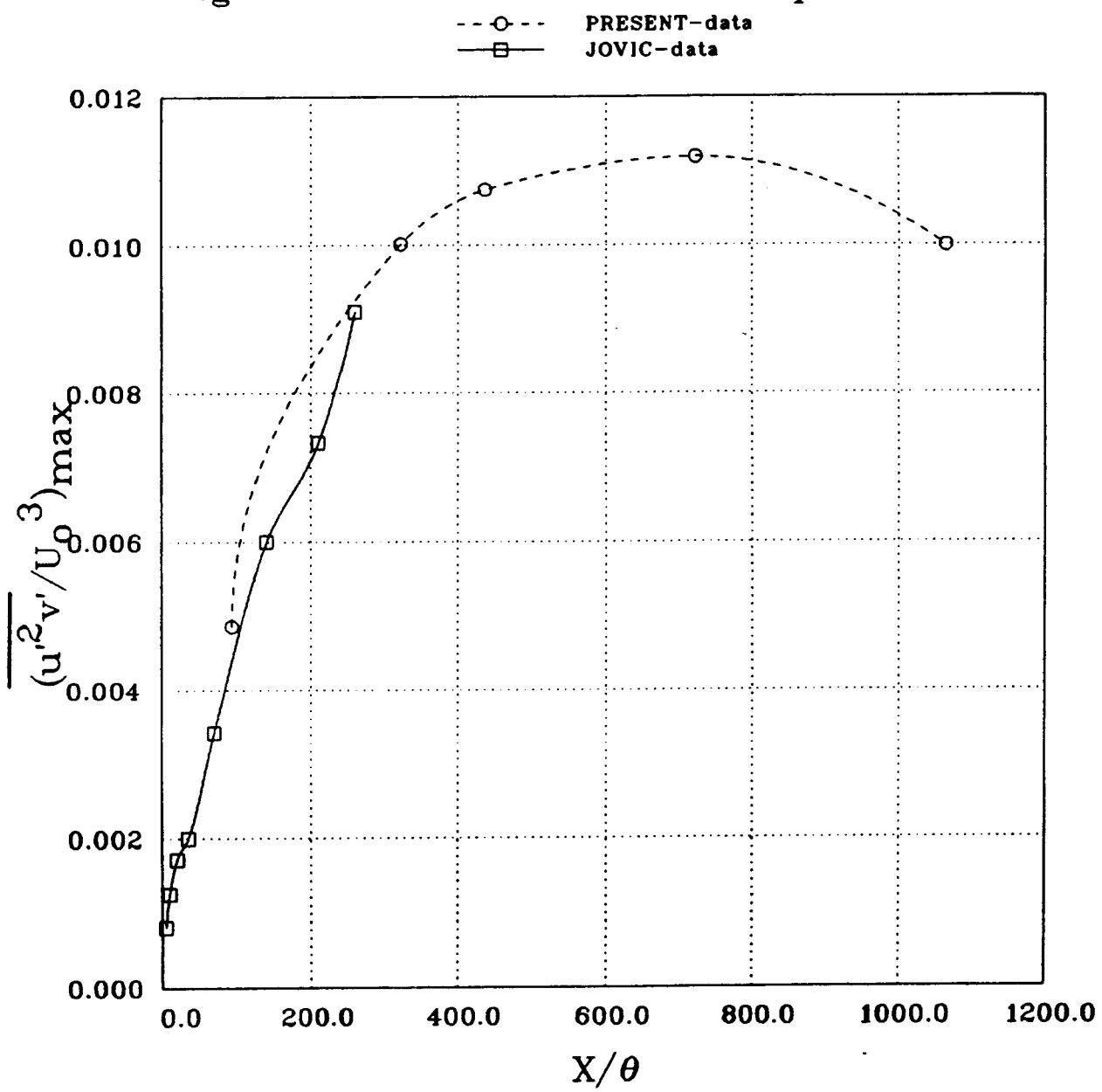

Figure 16: Plot of Maximum Triple Products

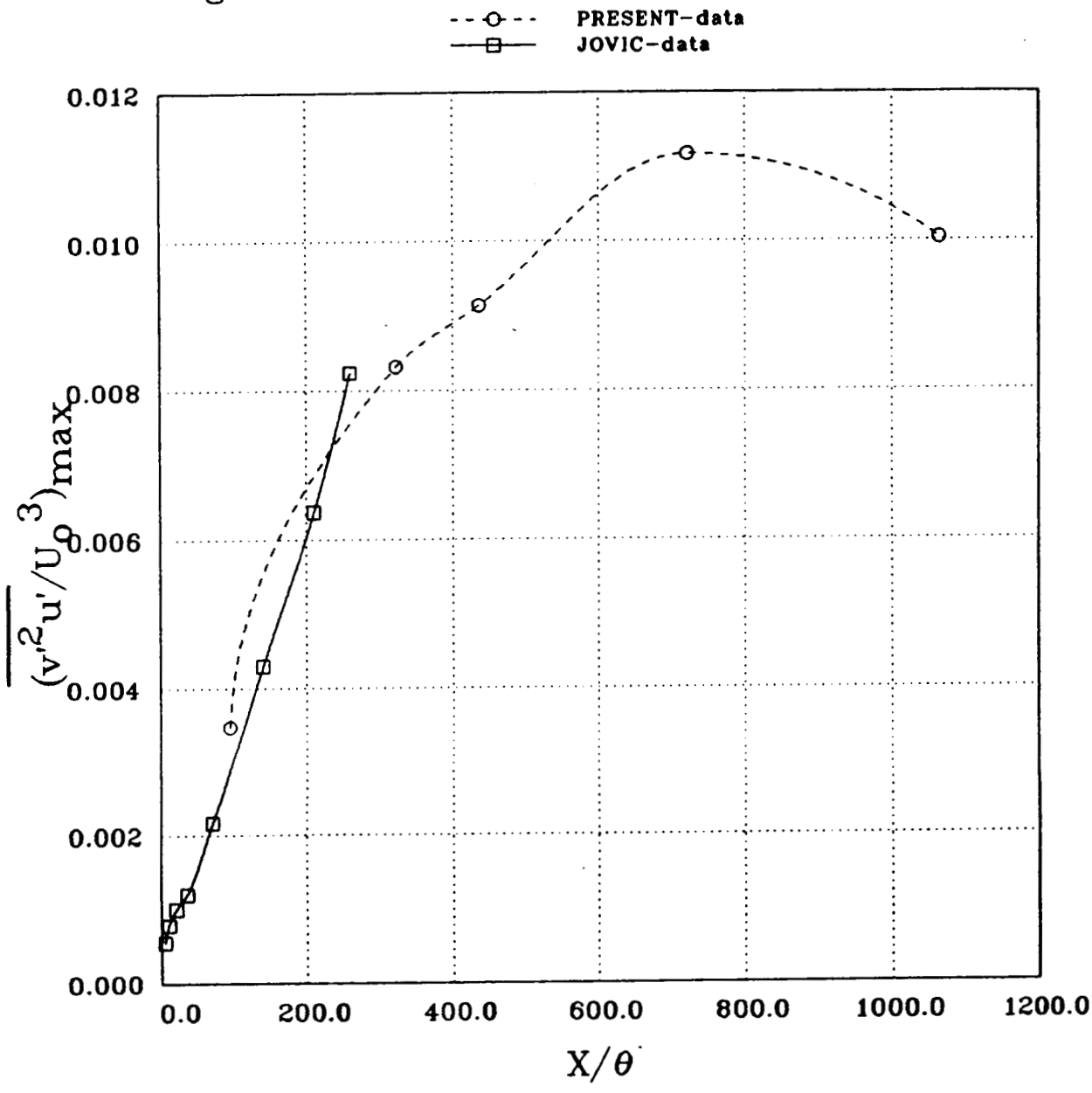

Figure 17: Plot of Maximum Fluctuation Profiles